Neointimal coverage of sirolimus-eluting stents at 6-month follow-up: evaluated by optical coherence tomography

Matsumoto, Daisuke ; Shite, Junya ; Shinke, Toshiro ; Otake, Hiromasa ; Tanino, Yusuke ; Ogasawara, Daisuke ; Sawada, Takahiro ; Oscar Luis…

(Citation)
European Heart Journal,28(8):961-967

(Issue Date)
2007-04

(Resource Type)
journal article

(Version)
Accepted Manuscript

Neointimal Coverage of Sirolimus-Eluting Stents at Six-Month Follow-Up – Evaluated by Optical Coherence Tomography

Running title: Sirolimus-eluting stents follow-up with OCT

Daisuke Matsumoto M.D., Junya Shite M.D., Toshiro Shinke M.D., Hiromasa Otake M.D., Yusuke Tanino M.D., Daisuke Ogasawara M.D., Takahiro Sawada M.D., Oscar Luis Paredes M.D., Ken-ichi Hirata M.D., Mitsuhiro Yokoyama M.D.

Kobe University Graduate School of Medicine, Division of Cardiovascular and Respiratory Medicine, Department of Internal Medicine

Address for correspondence:

Junya Shite M.D.

Associate Professor,

Kobe University Graduate School of Medicine, Division of Cardiovascular and Respiratory Medicine, Department of Internal Medicine

7-5-1 Kusunoki-cho, Chuo-ku, Kobe, Hyogo, 650-0017, Japan

Fax:81-78-382-5859, Tel:81-78-382-5846, E-mail:shite@med.kobe-u.ac.jp

Total words: 4530 words

No conflict of interest exists in connection with this article.

Abstract

Aims Since the intravascular ultrasound (IVUS) cannot detect neointimal layers in the majority of sirolimus-eluting stents (SES) at the chronic phase, it is still controversial to what extent SES remain uncovered. However, optical coherence tomography (OCT) with excellent resolution may be able to detect thinner neointima.

Methods and Results A total of 34 patients (57 SES) underwent OCT and IVUS evaluations at six-month follow up. The thickness of neointima on each SES strut cross section and strut apposition to the vessel wall were evaluated. By OCT evaluation**,** the median (25 th, 75 th percentiles) neointima thickness was 52.5 μm (28.0 μm, 147.6 μm) and the prevalence of struts covered by thin neointima undetectable by IVUS, was 64%. The average rate of neointima-covered struts in an individual SES was 89%. Nine SES (16%) showed full coverage by neointima, while the remaining stents had partially uncovered strut lesions. Among the 6840 struts visualized by OCT in all of the SES, 79 struts showed malapposition without neointimal coverage, and were frequently observed in the areas of SES overlap.

Conclusion At six months**,** most of the SES were covered with thin neointima, but few showed full coverage. **193 words**

Key Words: sirolimus-eluting stents; optical coherence tomography; neointima; malapposition

Introduction

Results of large-scale clinical trials have established that sirolimus-eluting stents (SES) inhibit neointimal proliferation and reduce in-stent restenosis [1], although the inhibition of stent re-endothelialization may increase susceptibility to late thrombosis. There have been reports that thrombosis occurred in SES after discontinuation of antiplatelet therapy and more than 1 year after implantation [2-4], a relatively rare occurence in bare metal stents (BMS). Interest has developed in the classification of a lack of neointimal coverage as a chronic condition. A recent intravascular ultrasound (IVUS) study found that intimal hyperplasia is not visible on most SES even at long-term follow-up [5]. The question whether the inability of IVUS to visualize neointima on SES results from an actual tissue deficit or from the limitation of IVUS resolution remained unanswered. A recent study by Kotani et al reported that the use of angioscopy resulted in frequent observations of transparent neointima on SES 3 to 6 months after stent implantation, suggesting the presence of thin neointimal coverage in SES which IVUS can not detect [6]. Angioscopy is indeed an important tool for visual qualification, but it can not quantify the proportion and thickness of the neointimal coverage.

Optical coherence tomography (OCT) is a new imaging modality that visualizes the intra-coronary features with high axial resolution (10-20μm) which is far better than IVUS resolution (100-150μm), even though the penetration depth of OCT is limited (1.25mm),

which is inferior to that of IVUS (5mm)[7]. Kume et al reported that OCT visualized apposition of stent struts and neointima formation in a cadaver specimen that could not be visualized completely by IVUS [8]. We therefore speculated that OCT may provide more precise information about neointimal proliferation on SES struts and make it possible to quantify the thickness of tissue on the surface of the stent struts. In the study reported here, we performed OCT examinations 6 months after SES deployment for a precise evaluation of neointimalization in SES struts at the chronic stage. These findings may provide important information about chronic SES status.

Methods

Study populations and methods

Between August 2004 and April 2005, 194 patients underwent percutaneous coronary intervention (PCI). BMS was implanted in 116 patients, because 70 had acute coronary syndrome, and 46 patients had to have non-cardiac surgery or an invasive examination soon after PCI. Another 22 patients underwent PCI without the stent (20 cases of balloon angioplasty and one each of directional atherectomy and rotablator). The remaining 56 patients received 105 SES (CYPHER^{TM}, Cordis Corp, Miami Lakes, FL, USA) implantations electively at our hospital. Every patient took 100mg aspirin at least 1 week before intervention, and 200mg ticlopidine immediately after SES deployment. This study

was approved by the ethical committee of Kobe University and all the patients enrolled in the study gave their written informed consent.

Prior to SES implantation, IVUS was performed using Atlantis SR Pro^{TM} catheters (Boston Scinentific, Natrick, MA, USA) with an automatic pullback device at 0.5 mm/sec to measure the vessel size and to identify the location of the plaque. After the stent implantation, IVUS was performed again to ensure the SES was fully expanded and well-apposed to the vessel wall. If not, additional high-pressure balloon expansion was repeated until examination of the IVUS indicated that the SES was well-apposed.

After each successful intervention, ticlopidine was discontinued after 3 months but aspirin therapy was maintained on a life-long basis. After six months, 20 patients did not consent to the invasive examination and the remaining 36 patients (64%) (60 SES) underwent the follow-up angiography and IVUS in the same manner as before. These patients became the candidate for an OCT examination.

IVUS analysis

Quantitative IVUS analysis was performed using commercially available soft ware (NetraIVUS^{TM}, ScImage, Los Altos, CA, USA). Before stent implantation, the lumen area and external elastic membrane (EEM) area were measured. After stent implantation, final EEM area and smallest SES area were measured for the proximal, mid and distal portion of the stented segments. At the six-month follow-up, the EEM area, SES area and percentage of

the neointimal area, which was defined as the largest neointimal area divided by the SES area, were evaluated.

OCT examination

With the aid of a 6F guiding catheter, an over-the-wire type occlusion balloon catheter （Helios^{TM}, LightLab Imaging Inc., Westford, MA, USA） was advanced into the distal end of the SES implantation site under guidance by a 0.014 inch angioplasty wire. The guide wire was then removed and the OCT imaging probe (ImageWire^{TM}, LightLab Imaging Inc.) was inserted through the over-the-wire lumen of the occlusion balloon. With the ImageWire held in place, the occlusion balloon was withdrawn until proximal to the SES. To clear blood from the imaging site, the occlusion balloon was inflated to 0.6 atm and Lactated Ringer's solution was infused into the coronary artery from the distal tip of the occlusion balloon at 0.5 ml/sec. The entire length of the stent was imaged with an automatic pullback device moving at 1mm/sec and the OCT image clearly visualized the stent cross-section.

OCT analysis

OCT images were analyzed by two independent observers who were blinded to the clinical presentations and lesion characteristics and used proprietary off-line soft ware provided by LightLab Imaging Inc. The OCT image of each stent strut was classified into one of three categories: (1) well-apposed to vessel wall with apparent neointimal coverage,

(2) well-apposed to vessel wall without neointimal coverage and (3) malapposed to the vessel wall without neointimal coverage. A stent strut was classified as malapposed when the distance between its inner surface reflection and the vessel wall was greater than 150 μm. This criterion was determined by adding the OCT axial resolution (20 μm) to the actual thickness of an SES strut (130 μm). If the two observers disagreed, a consensus diagnosis was obtained with repeated off-line readings. Representative images of the three strut categories are shown in Figure 1.

If neointimal coverage on the strut was observed, its average thickness was measured. The potential factors that predispose SES to malapposition –chronic total occluded (CTO) vs non-CTO vessel, implantation in de novo lesions vs previously stented restenosed lesions, and SES overlapping vs non-overlapping areas - were noted. In addition, the frequency of thrombus formation in SES was recorded with a thrombus as observed in the OCT image defined as an irregular mass protruding into the lumen, and measuring ≥250μm at its thickest point [9].

Statistical analysis

Qualitative data are presented with frequencies and quantitative data are shown as medians (25 th, 75 th percentiles) or mean values ± SD as indicated**.** Comparison of the frequencies of malapposition between the two groups was performed with the chi-square test.

To assess the inter-observer and intra-observer variabilities, the results were compared using the κ-test of concordance for the categorical data and data of continuous variables were entered into a Bland-Altman plot. A two-sided p-value of less than 0.05 was considered statistically significant.

Results

Of the 36 cases that underwent follow-up angiography, OCT images could not be obtained for two cases, one because of contraindication involving occlusion of coronary flow in a left main trunk lesion, and other because of the inability to place the occlusion balloon in a severely calcified tortuous vessel. In the other 34 cases (57 SES), clear OCT images were obtained without any complications. Table 1 shows the baseline characteristics of the study subjects consisting of patients with angina pectoris (24 cases) and old myocardial infarction (10 cases). Twenty-eight patients received SES treatment for de novo lesions, and six each for in-stent restenosis (SES-in-BMS), and for CTO vessels. The average interval of follow-up angiography was 202 days. The size of SES ranged from 2.5mm to 3.5mm diameter and 13mm to 28mm length and there were two angiographic in-stent restenoses (>50% occlusion) with focal neointimal proliferation.

IVUS data

EEM and SES areas are shown in Table 2. An SES area of more than 6 mm^2 was attained

and after 6 months the EEM and SES areas had not changed significantly. As for the percentage of the neointimal area, it accounted for only 0-10 % in 81% of the SES, because most of the neointima could not be detected by IVUS (Figure 2).

Neointimal thickness on SES struts by OCT image.

Figure 3 shows representative IVUS and OCT images, obtained at the same distance from a major side branch, of an SES displaying neointimal coverage. At follow-up IVUS examination, the presence of echo side lobes and insufficient resolution precluded quantification of neointimal thickness on the struts. On the other hand, OCT could visualize stent strut cross sections and clearly showed the presence of surface neointima. In total, OCT visualized 6840 stent strut cross sections in 57 SES and made quantification possible of the neointimal thickness on each strut. According to the Bland-Altman analysis, the mean difference in neointimal thickness for intra-observer measurements was 2.3 μm (upper 2SD: 29.6 μm and lower 2SD: -25.1 μm), and that for inter-observer measurements was 0.7 μm (upper 2SD:31.5 μm, lower 2SD: -33.7 μm). The median thickness of neointima on a SES strut was 52.5 μm (25 th: 28.0 μm, 75 th: 147.6 μm). The prevalence of stent struts covered by thin neointima of less than 100 μm thickness, which is beyond IVUS resolution, was 64%. (Figure 4).

Classification of stent strut condition in relation to neointimal proliferation

Inter-observer and intra-observer variabilities for the classifications of strut conditions were κ=0.75 and κ = 0.82, respectively.

Of the 6840 stent struts in 57 SES, 70 (1%) were located at a major side branch and all of these were separated from the vessel wall. Of the remaining 6770 struts, 6236 (91%) were classified as well-apposed with neointima, 455 (7%) as well-apposed without neointima and 79 (1%) as malapposed without neointima (Figure 5).

A comparison of all individual stents showed that nine SES (16%) featured full coverage of every strut by neointima, while the remaining 48 stents contained partially uncovered strut lesions. Individual SES showed the following frequencies: 89% had well-apposed struts with neointima; 8% well-apposed struts without neointima; 2% mallapposed struts without neointima; and 1% a side branch site.

Factors affecting malapposition

According to the vessel characteristics before stent deployment, the frequency of SES malapposition in CTO vessels, 36 / 1395 struts (2.6%), was higher than that in non-CTO vessels, 43 / 5375 struts (0.8%) ($p<0.0001$). Overlapping SES struts showed malapposition more frequently, 29 / 362 struts (8.0%), than did non-overlapping SES struts, 50 / 6408 struts (0.8%) ($p<0.0001$) (Figure 6). In contrast, SES implanted in BMS restenosed lesions showed significantly less malapposition, 7 / 1213 struts (0.6%), than in SES for de novo lesion, 72 /

5557 struts (1.3%) (p=0.0496). Representative images of SES malapposition in a CTO lesion, SES malapposition in a segment with two overlapping stents, and a well-apposed SES in BMS restenosis are shown in Figure 7.

Thrombus attachment to SES

We detected three SES with apparent thrombus formation attached to the stent struts. One was located at a stent fracture[10], and the others were at non-fractured sites adjacent to malapposed struts (Figure 8). However, none of these cases showed any evidence of thrombotic events.

Discussion

This is the first systematic study of SES follow-up using the high-resolution capabilities of OCT imaging. OCT demonstrated its ability to visualize the thin neointima on each stent strut and quantify its thickness. Our study's results indicate that the majority (64%) of SES struts were covered by a thin neointima layer less than 100 μm thick, which is beyond the capacity of IVUS to detect. In addition, OCT imaging disclosed that almost 90 % of the individual stent struts were covered with neointima. However, only a few SES showed full coverage by neointima, with the remaining stents displaying partially uncovered strut lesions.

Stent thrombosis usually results in ST segment elevation myocardial infarction or death. A matter of concern is that SES are susceptible to late thrombosis related to delayed re-endothelialization of the stent struts. Following an SES implantation, antiplatelet therapy typically consists of ticlopidine or clopidogrel for more than 3 months and life-long aspirin, based on an empirical protocol. As long as the standard antiplatelet therapy is continued, the real-world data of SES will show the same frequency of stent thrombosis as that in BMS [1].

However, for the increasing numbers of patients with implanted SES, the issue of whether antiplatelet therapy can be discontinued before surgery or invasive examinations remains unresolved. In the case of BMS, Wilson et al reported that discontinuation of antiplatelet therapy later than 6 weeks was relatively safe for noncardiac surgery [11]. Ueda et al found by using angioscopy, that neointimal coverage of BMS is completed within 3 months after implantation [12]. For SES, however, no major studies have been reported to predict when neointimal coverage will be attained after SES implantation.

In our OCT study of SES, a significant percentage of uncovered SES struts was found six months after implantation, indicating that re-endothelialization was suppressed. Although the prevalence of uncovered struts identified by OCT examination was less frequent than IVUS examination alone would indicate, we could not conclude that complete cessation of antiplatelet therapy for SES at six months is safe.

In spite of our protocol of life-long aspirin and three-month ticlopidine, three thrombi

attached to SES were detected, one was at a stent fracture site [10] and the other two adjacent to malapposed struts. This leads us to speculate that stent struts uncovered by neointima and persistently separated from the vessel wall may be thrombogenic. This speculation is supported by a recent report that angioscopy disclosed that thrombi were commonly seen in SES incompletely covered with neointima [6]. To determine a safe antiplatelet protocol, continued surveillance for SES late thrombosis is mandatory, especially following any discontinuation of dual antiplatelet therapy. However, because the stent thrombosis rate is very small (0.6% in SES [1]), a larger-scale study is required.

In our OCT study, the prevalence of malapposition without neointimal coverage was less than 2%. The causes of stent malapposition have been reported elsewhere as underexpansion at implantation, stent recoil, decrease of plaque volume and vessel positive remodeling [13-16]. Our IVUS results show that the average areas of EEM and SES did not change significantly during 6 months after implantation. Thus, the mechanism of malapposition detected by OCT at 6 months may not be simply due to positive vessel remodeling or stent shrinkage. The lesion-specific mechanism of malapposition needs to be examined in more detail by binary OCT examinations. Although we could perform the OCT examination only at follow-up, the predisposing factors for SES malapposition which could be identified included a CTO vessel and SES overlapping segments. We hypothesize that the mechanism for the increased malapposition in a CTO lesion may involve the absorption of mural thrombus accompanied

by suppressed neointimal hyperplasia. Furthermore, the malapposition in SES overlapping segments may be associated with excess inhibition of neointimal hyperplasia due to the double dose of sirolimus. This hypothesis is supported by the study of Finn et al, in which overlapping stent segments exhibited a delayed healing process compared with proximal and distal non-overlapping segments in animals [17]. Thus, to avoid late malapposition, the length of any unavoidable SES overlap should be minimized. In addition, our study showed less malapposition for SES implanted in BMS restenosis. We speculate that the abundant neointimal growth inside the BMS prior to SES implantation may prevent malapposition of the SES, and that sirolimus may still exert its inhibitory effect on excessive neointimal hyperplasia in the stents. This agrees with previous reports indicating SES is effective for in-stent restenosis treatment and for reducing re-restenosis, with no evidence of malapposition [18-20].

Limitations

In our study, the efficacy of OCT was limitated in terms of imaging certain lesions, such as ostial lesions due to the risk of producing a blood-free environment. Also, severely calcified tortuous vessels could not be imaged with OCT due to the difficulty of passing through the lesion with the occlusion balloon. Thus, our study results do not represent an unbiased sampling of all patients who received SES implantations, with the nature of SES in

ostial lesions in particular remaining to be clarified.

Several previous studies have established methods for tissue characterization with OCT, including differentiation of fibrous tissue, lipid and calcium plaque composition and the presence of thrombus in the lumen [9,21]. We diagnosed the tissue surrounding SES as neointima because of its isodensity with the coronary intima. Sousa et al reported that necropsy findings 4 years after implantation of SES showed >95% of the stent strut surfaces were endothelialized [22]. This neointima consisted of smooth muscle cells and macrophages in a collagen-rich matrix. Additional studies comparing the appearance of cadaver specimens on OCT images with histological verification are needed to confirm the ability of OCT to determine the composition of neointima.

Because the resolution of OCT is 15-20 μm, tissue structures with dimensions less than 15 μm, such as endothelium, cannot be resolved with OCT. The possibility can therefore not be excluded that OCT images of uncovered SES struts may not be completely devoid of tissue growth. To the best of our knowledge, however, there is no evidence that endothelium covers stent struts without neointimal growth. Finn et al, using scanning electron microscope, reported that at overlapping drug-eluting stent sites, most of the stent struts looked uncovered by endothelial cells [17]. Thus, a certain proportion of SES struts may be devoid of tissue coverage and should thus have thrombogenic potency.

Conclusions

We conclude that OCT is a powerful modality for visualizing the thin neointima covering SES struts. At six-month follow-up, most of the SES were found to be covered with thin neointima, but few of the SES showed full coverage. To minimize the potential for stent malapposition devoid of neointima coverage, any overlap between adjacent SES should be as short as possible to minimize the potential for late thrombosis. To determine when neointima covers the whole SES, thus warranting discontinuation of antiplatelet therapy, extended long term follow-up with OCT may be helpful.

References

1. Babapulle MN, Joseph L, Belisle P, Brophy JM, Eisenberg MJ. A hierarchical Bayesian meta-analysis of randomized clinical trials of drug-eluting stents. Lancet. 2004; 364: 583-591.

2. McFadden EP, Stabile E, Regar E, Cheneau E, Ong ATL, Kinnaird T, Suddath WO, Weissman NJ, Torguson R, Kent KM, Pichard AD, Satler LF, Waksman R, Serruys PW. Late thrombosis in drug-eluting coronary stents after discontinuation of antiplatelet therapy. Lancet. 2004; 364: 1519-1521.

3. Jeremias A, Sylvia B, Bridges J, Kirtane AJ, Bigelow B, Pinto DS, Ho KK, Cohen DJ, Garcia LA, Cutlip DE, Carrozza JP Jr. Stent thrombosis after successful sirolimus-eluting stent implantation. Circulation 2004; 109: 1930-1932.

4. Orlic D, Bonizzoni E, Stankovic G, Airoldi F, Chieffo A, Corvaja N, Sangiorgi G, Ferraro M, Briguori C, Montorfano M, Carlino M, Colombo A. Treatment of multivessel coronary artery disease with sirolimus-eluting stent implantation: immediate and mid-term results. J Am Coll Cardiol 2004; 43: 1154-1160.

5. Sonoda S, Morino Y, Ako J, Terashima M, Hassan AHM, Bonneau HN, Leon MB, Moses JW, Yock PG, Honda Y, Kuntz RE, Fitzgerald PJ for the SIRIUS Investigators. Impact of final stent dimensions on long-term results following Sirolimus-eluting stent implantation. Serial intravascular ultrasound analysis from the SIRIUS trial. J Am Coll Cardiol 2004; 43:

1959-1963.

6. Kotani J, Awata M, Nanto S, Uematsu M, Oshima F, Minamiguchi H, Mintz GS, Nagata S. Incomplete neointimal coverage of sirolimus-eluting stents Angioscopic findings. J Am Coll Cardiol 2006; 47: 2108-2111.

7. Jang IK, Bouma BE, Kang DH, Park SJ, Park SW, Seong KB, Choi KB, Shishkov M, Schlendorf K, Pomerantsev E, Houser SL, Aretz T, Tearney GJ. Visualization of coronary atherosclerotic plaques in patients using optical coherence tomography: comparison with intravascular sound. J Am Coll Cardiol 2002; 39: 604-609.

8. Kume T, Akasaka T, Kawamoto T, Watanabe N, Toyota E, Sukmawan R, Sadahira Y, Yoshida K. Visualization of neointima formation by optical coherence tomography. Int Heart J. 2005; 46: 1133-1136.

9. Jang IK, Tearney GJ, MacNeill B, Takano M, Moselewski F, Iftima N, Shishkov M, Houser S, Aretz HT, Halpern EF, Bouma BE. In vivo characterization of coronary atherosclerotic plaque by use of optical coherence tomogoraphy. Circulation 2005; 111: 1551-1555.

10. Shite J, Matsumoto D, Yokoyama M. Sirolimus-eluting stent fracture with thrombus, visualization by optical coherence tomography. Eur Heart J 2006; 27: 1389.

11. Wilson SH, Fasseas P, Orford JL, Lennon RJ, Horlocker T, Charnoff NE, Melby S, Berger PB. Clinical outcome of patients undergoing non-cardiac surgery in the two months

following coronary stenting. J Am Coll Cardiol 2003; 42: 234-240.

12. Ueda Y, Nanto S, Komamura K, Kodama K. Neointimal coverage of stents in human coronary arteries observed by angioscopy. J Am Coll Cardiol 1994;23:341-346.

13. Shah VM, Mintz GS, Apple S, Weissman NJ. Background incidence of late malapposition after bare-metal stent implantation. Circulation 2002;106:1753-1755.

14. Mintz GS, Shah VM, Weissman NJ. Regional remodeling as the cause of late stent malapposition. Circulation 2003;107:2660-2663.

15. Hong MK, Mintz GS, Lee CW, Kim YH, Lee SW, Song JM, Han KH, Kang DH, Song JK, Kim JJ, Park SW, Park SJ. Incidence, mechanism, predictors, and long-term prognosis of late stent malapposition after bare-metal stent implantation. Circulation 2004; 109: 881-886.

16. Ako J, Morino Y, Honda Y, Hassan A, Sonoda S, Yock PG, Leon MB, Moses JW, Bonneau HN, Fitzgerald PJ. Late incomplete stent apposition after sirolimus-eluting stent implantation: a serial intravascular ultrasound analysis. J Am Coll Cardiol 2005; 46: 1002-1005.

17. Finn AV, Kolodgie FD, Harnek J, Guerrero LJ, Acampado E, Tefera K, Skorija K, Weber DK, Gold HK, Virmani R. Differential response of delayed healing and persistent inflammation at sites of overlapping sirolimus- or paclitaxel-eluting stents. Circulation 2005; 112: 270-278.

18. Sousa JE, Costa MA, Abizaid A, Sousa AGMR, Feres F, Mattos LA, Centemero M,

Maldonado G, Abizaid AS, Pinto I, Falotico R, Jaeger J, Popma JJ, Serruys PW. Sirolimus-eluting stent for the treatment of in-stent restenosis: a quantitative coronary angiography and three-dimensional intravascular ultrasound study. Circulation. 2003; 107: 24-27.

19 Degertekin M, Regar E, Tanabe K, Smits PC, Giessen WJ, Carlier SG, Feyter P, Vos J, Foley DP, Ligthart JMR, Popma JJ, Serruys PW. Sirolimus-eluting stent for treatment of complex in-stent restenosis: the first clinical experience. J Am Coll Cardiol. 2003;41:184-189.

20. Neumann FJ, Desmet W, Grube E, Brachmann J, Presbitero P, Rubartelli P, Mugge A, Pede FD, Fullgraf D, Aengevaeren W, Spedicato L, Popma JJ. Effectiveness and safety of sirolimus-eluting stents in the treatment of restenosis after coronary stent placement. Circulation. 2005;111:2107-2111.

21. Yabushita H, Bouma BE, Houser SL, Aretz T, Jang IK, Schlendorf KH, Kauffman CR, Shishkov M, Kang DH, Halpen EF, Tearney GJ. Characterization of human atherosclerosis by optical coherence tomography. Circulation 2002;106:1640-1645.

22. Sousa JE, Costa MA, Farb A, Abizaid A, Sousa A, Seixas AC, Silva LM, Feres F, Pinto I, Mattos LA, Virmani R. Vascular healing 4 years after the implantation of sirolimus-eluting stent in humans. Circulation 2004;110:e5-e6.

Figure Legends

Figure 1. Classification of sirolimus-eluting stents (SES) strut conditions by optical coherence tomography (OCT). (1): Well-apposed with neointimal coverage, (2): Well-apposed without neointimal coverage, (3): Malapposed without neointimal coverage.

Figure 2. Distribution of percentage of neointimal area (%NA) determined by intravascular ultrasound (IVUS) at the site of minimum lumen area of SES at 6-month follow-up.

Figure 3. Representative cross-sectional images of SES at six-month follow-up obtained at the same distance from a major side branch by IVUS and OCT.

Figure 4. Distribution of the thickness of neointima (NI) on SES struts. Median (25th, 75th percentiles) thickness was 52.5 μm (28.0, 147.6) and the prevalence of SES struts covered by neointima less than 100 μm thick, which is beyond IVUS resolution, was 64%.

Figure 5. Distribution of SES strut condition. Of the 6840 stent struts in 57 SES, 6236 (91%) were classified as well-apposed with neointima, 455 (7%) as well-apposed without neointima, 79 (1%) as malapposed without neointima and 70 (1%) were at the site of a major

side branch .

Figure 6. Factors predisposing SES malapposition. CTO indicates chronic total occlusion lesion.

Figure 7. OCT images of SES malapposition occurring under the following conditions: at CTO site (left panel), at SES overlapping site (middle panel), and at SES for bare metal stent (BMS) restenosis (right panel).

Figure 8. A case with thrombus (Th) presumed to have developed due to malapposed (Mal) struts in SES. Angiogram and OCT scanning.

Table 1. Patient Characteristics

Number	34 (Male: 27, Female: 7)	57 stents
Age (yrs)	66±10	
f/u (days)	202±23	
Disease (%)		
Angina pectoris	24 (71)	40 stents (70)
Old myocardial infarction	10 (29)	17 stents (30)
Risk factor (%)		
Hypertension	19 (56)	
Hyperlipidemia	23 (68)	
Diabetes mellitus	15 (44)	
Smoking	20 (59)	
Vessels LAD/LCX/RCA		28/ 14/ 15 stents
Lesion type (%)		
De novo	28 (82)	48 stents (84)
Restenosis	6 (18)	9 stents (16)
Chronic total occlusion	6 (18)	12 stents (21)

LAD, left anterior descending artery; LCX, left circumflex artery; RCA, right coronary artery

Table 2. Intravascular ultrasound analysis before and after stent implantation, and at 6-month follow-up.

	Pre-stenting		Post-stenting		Six-month follow-up	
	Lumen area	EEM area	SES area	EEM area	SES area	EEM area
Proximal (mm^2)	6.3±2.9	15.2±4.3	7.9±2.1	16.6±4.2	7.9±2.3	16.8±5.0
Mid (mm^2)	4.5±2.3	13.9±4.9	7.9±2.2	15.5±4.5	7.9±2.5	15.8±4.3
Distal (mm^2)	4.6±1.9	12.4±5.5	6.8±2.0	13.7±5.0	6.9±2.0	13.7±4.8

Proximal, mid and distal each refer to 1/3 segment of the stented lesion; EEM, external elastic membrane; SES, sirolimus-eluting stents.

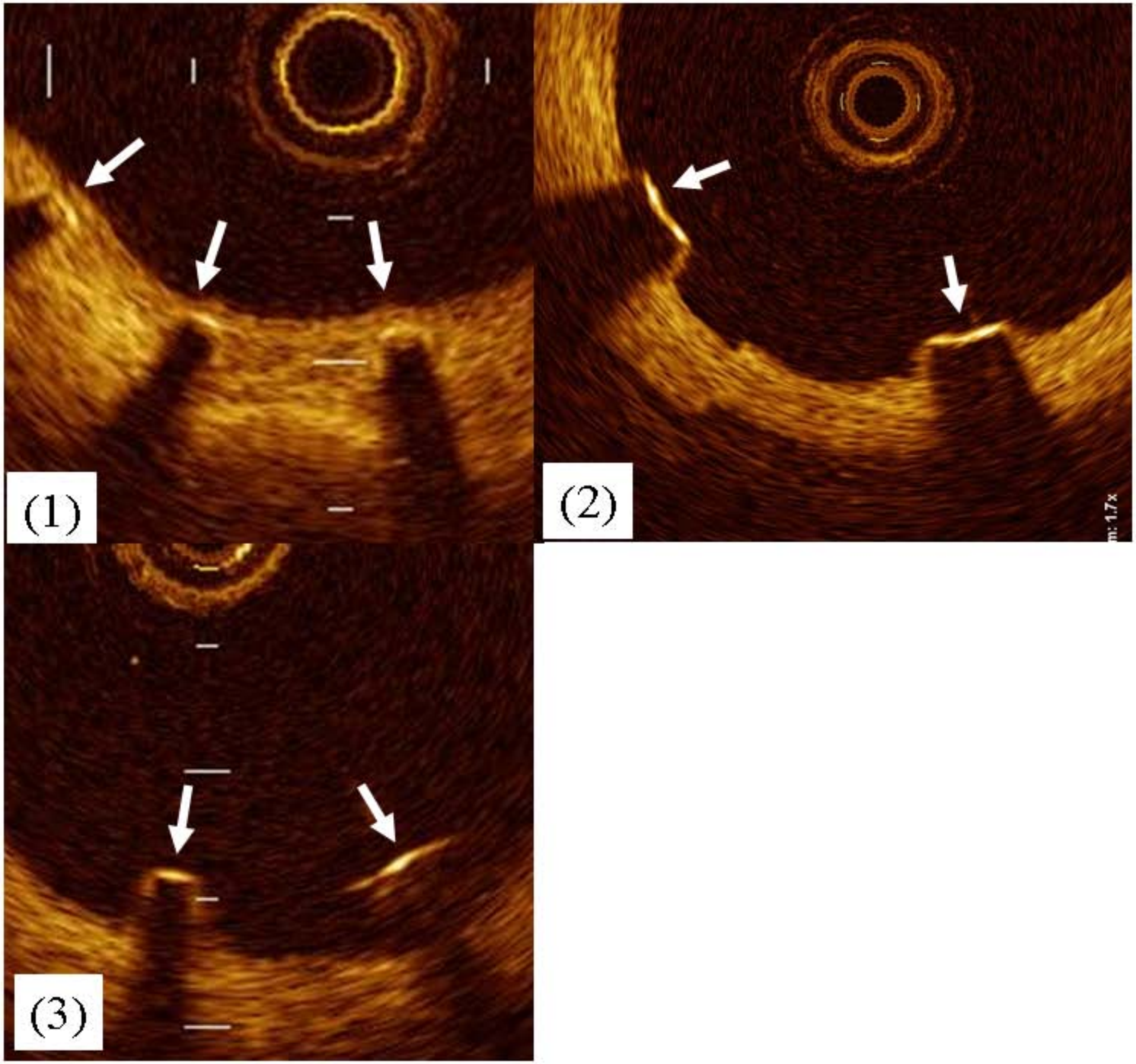
(1)
(2)
(3)

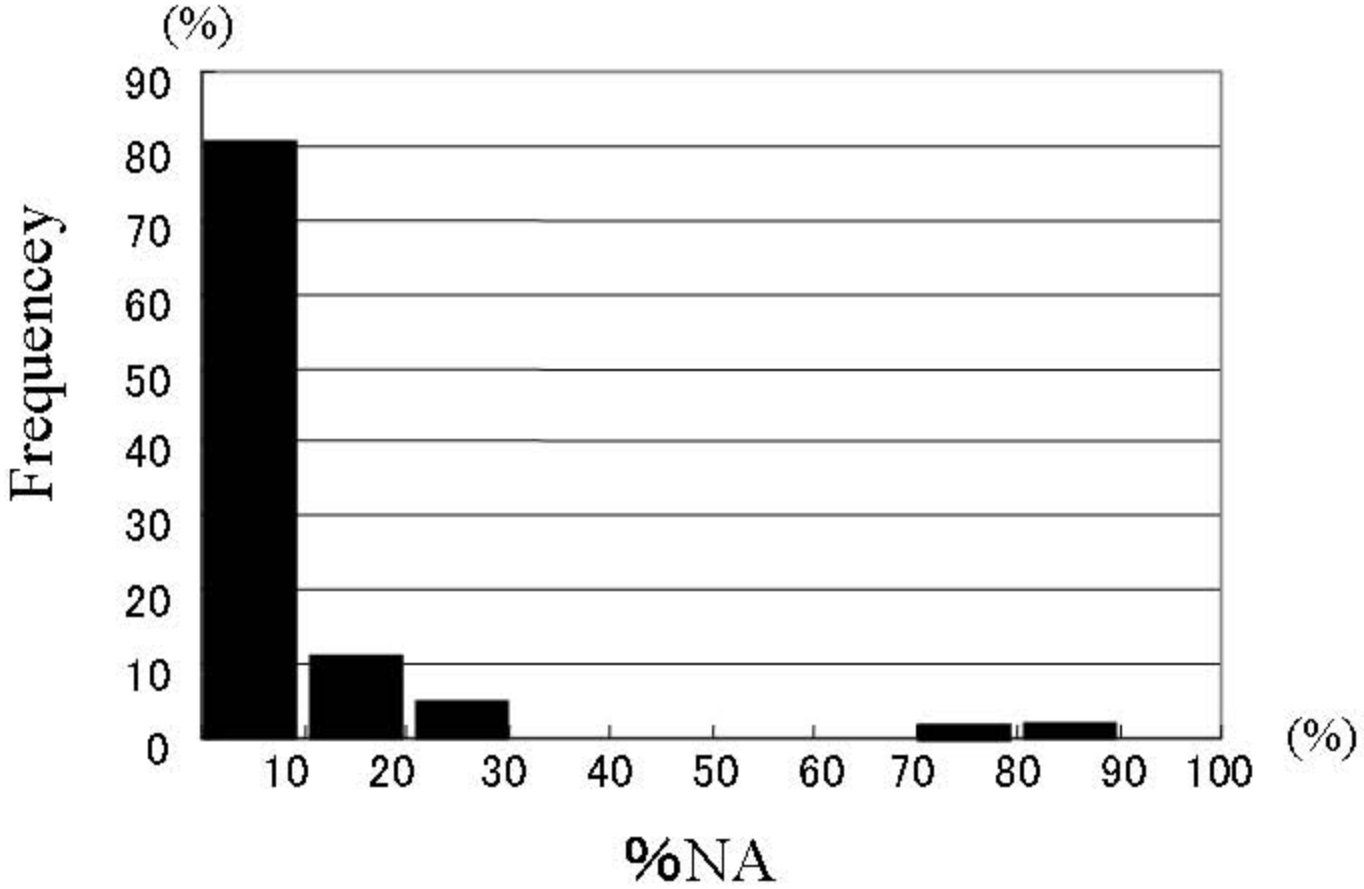
(%)
90
80
70
60
50
40
30
20
10
0
Frequencey
10
20
30
40
50
60
70
80
90
100
(%)
%NA

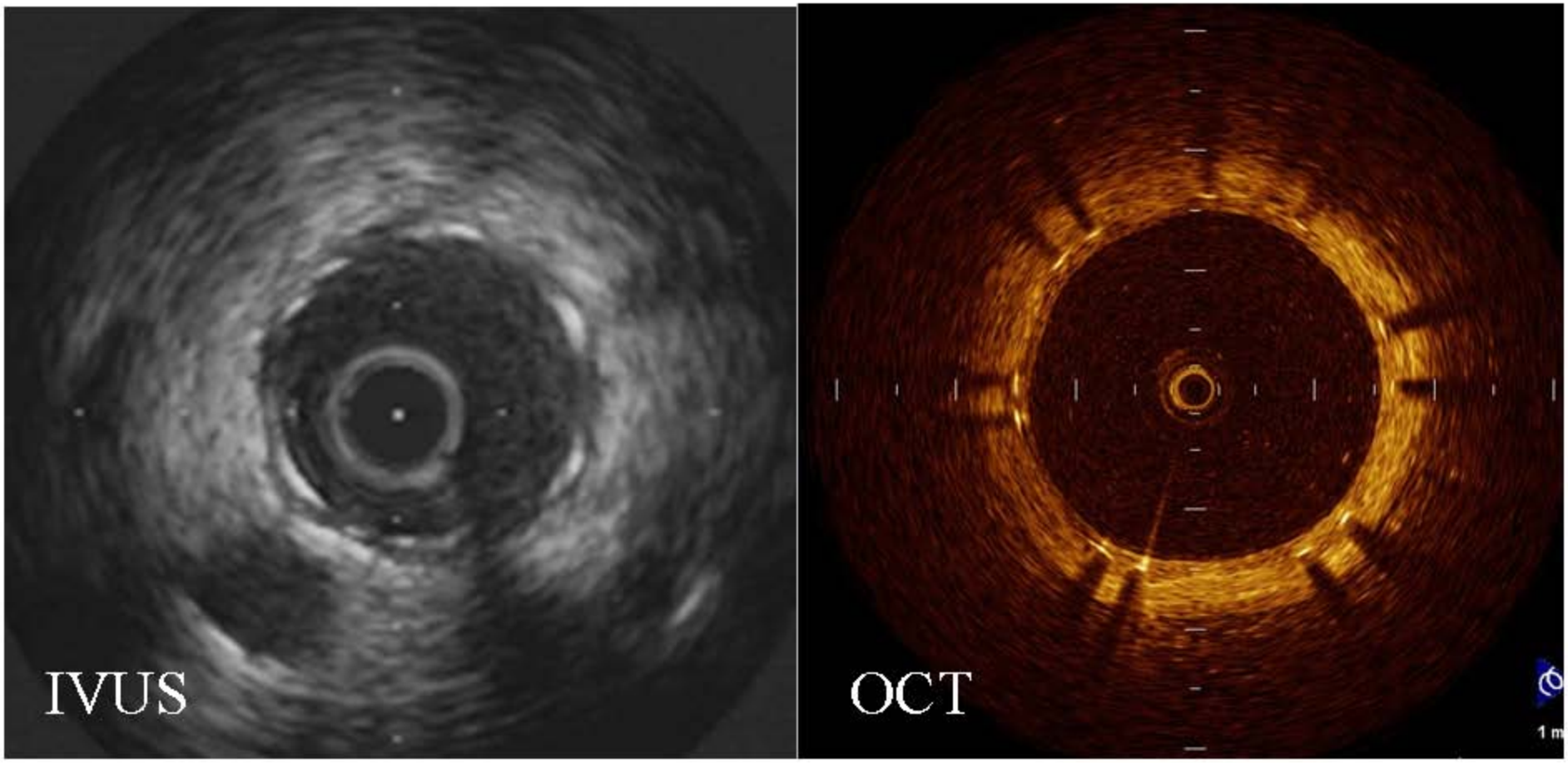
IVUS
OCT

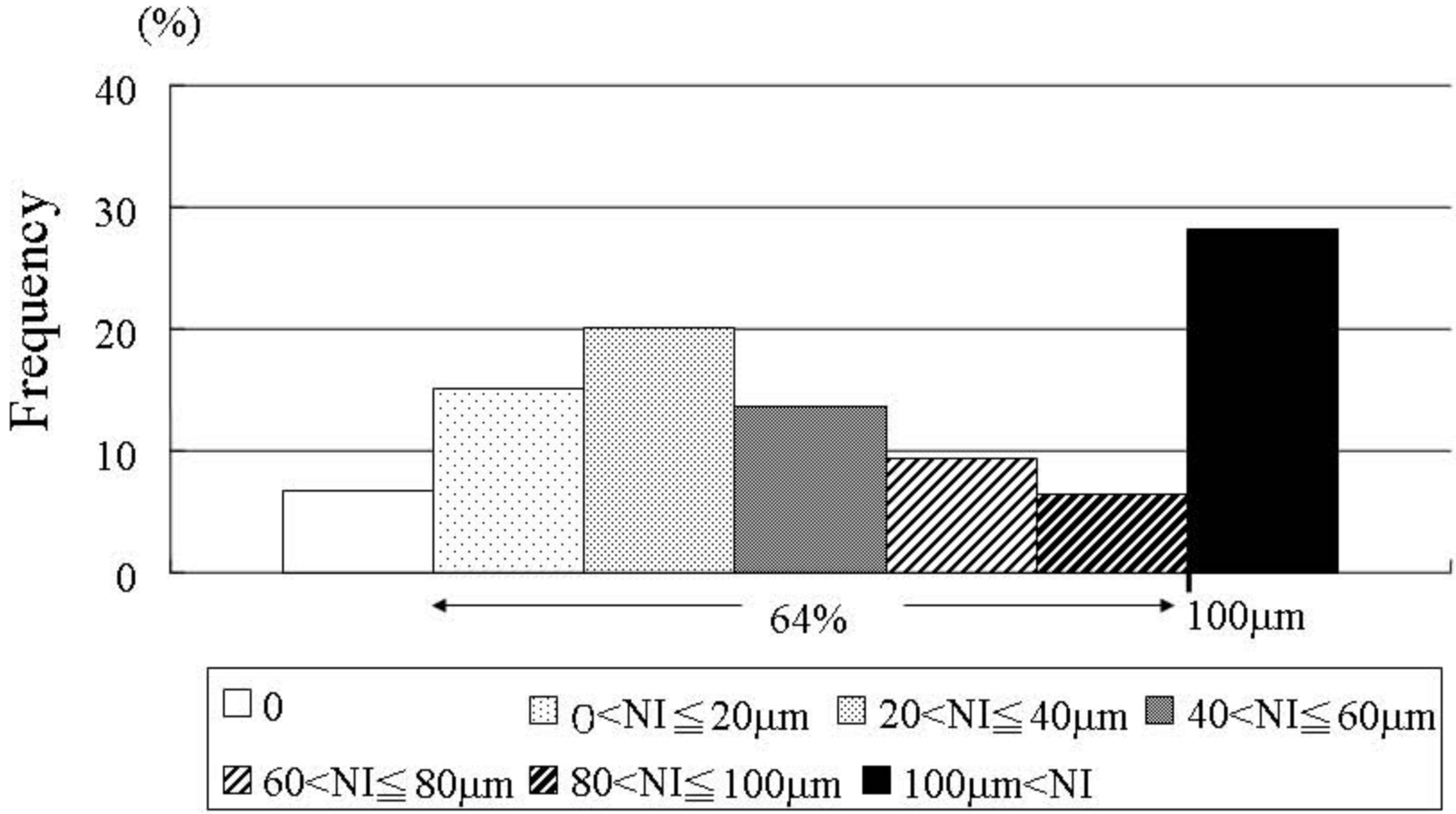
(%)
40
30
20
10
0
Frequency
64%
100μm
0
0<NI≦20μm
20<NI≦40μm
40<NI≦60μm
60<NI≦80μm
80<NI≦100μm
100μm<NI

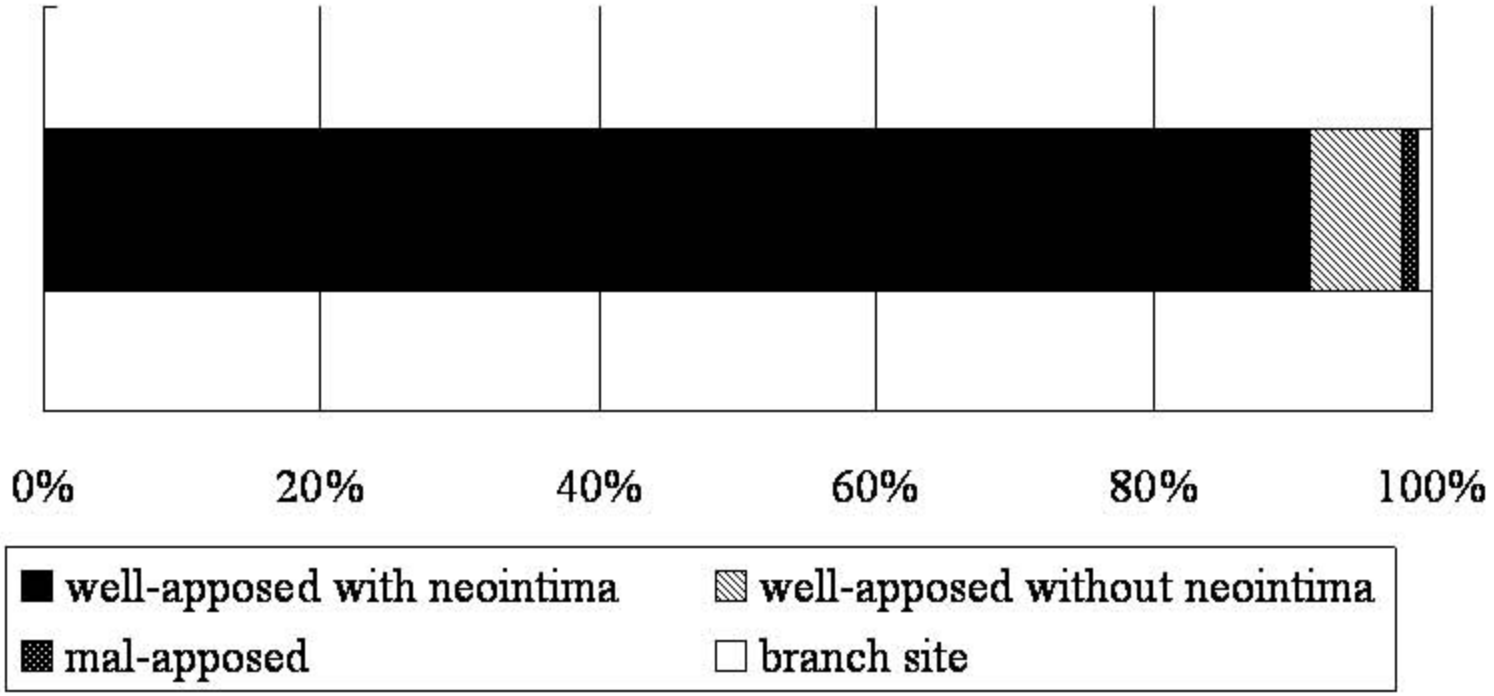
0%
20%
40%
60%
80%
100%
well-apposed with neointima
well-apposed without neointima
mal-apposed
branch site

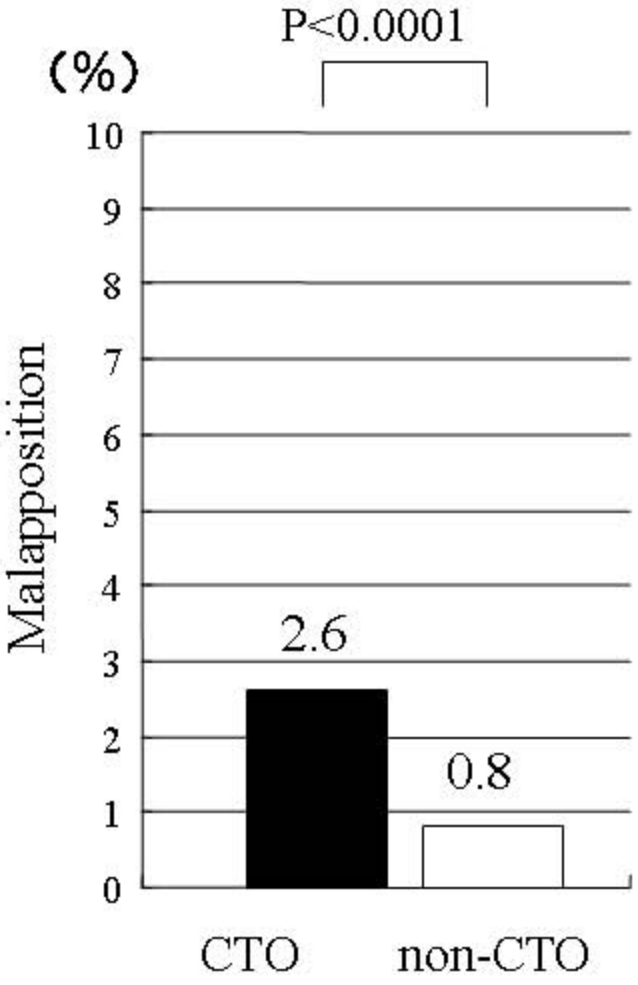
P<0.0001
(%)
Malapposition
10
9
8
7
6
5
4
3
2
1
0
2.6
0.8
CTO
non-CTO

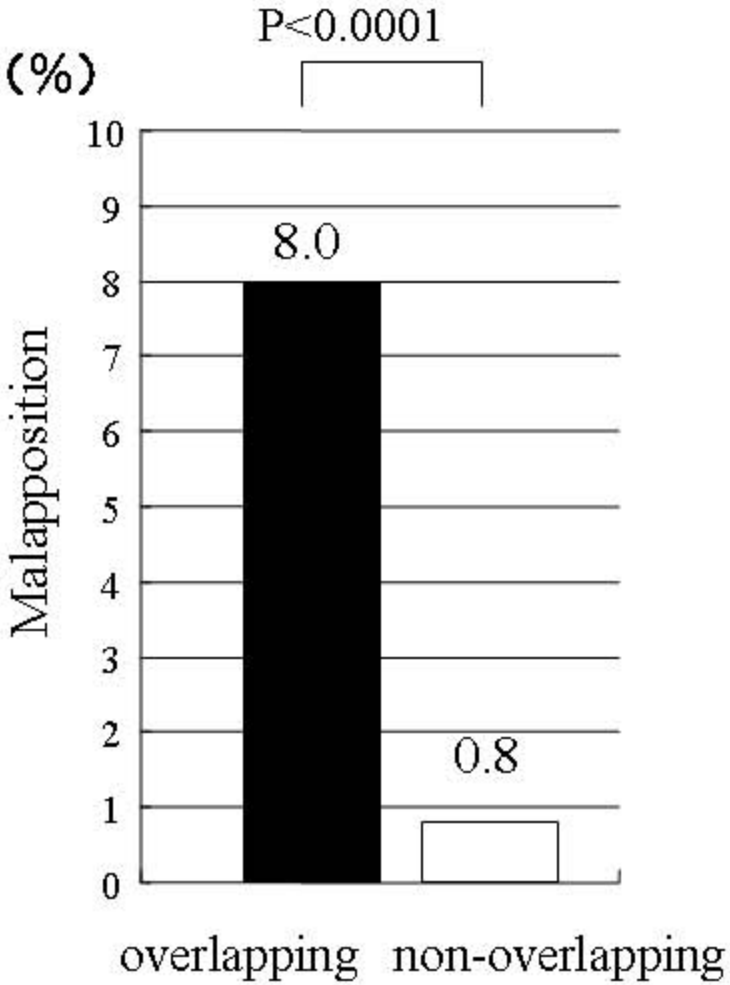
P<0.0001
(%)
Malapposition
10
9
8
7
6
5
4
3
2
1
0
8.0
0.8
overlapping
non-overlapping

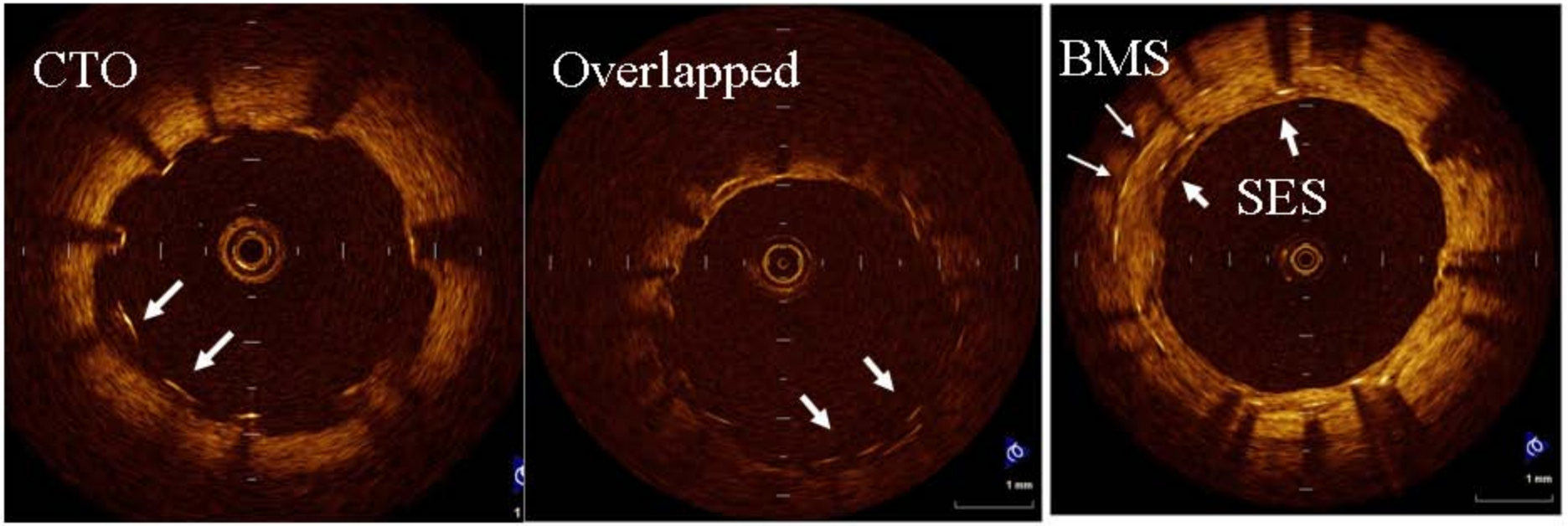
CTO
Overlapped
BMS
SES
1 mm
1 mm

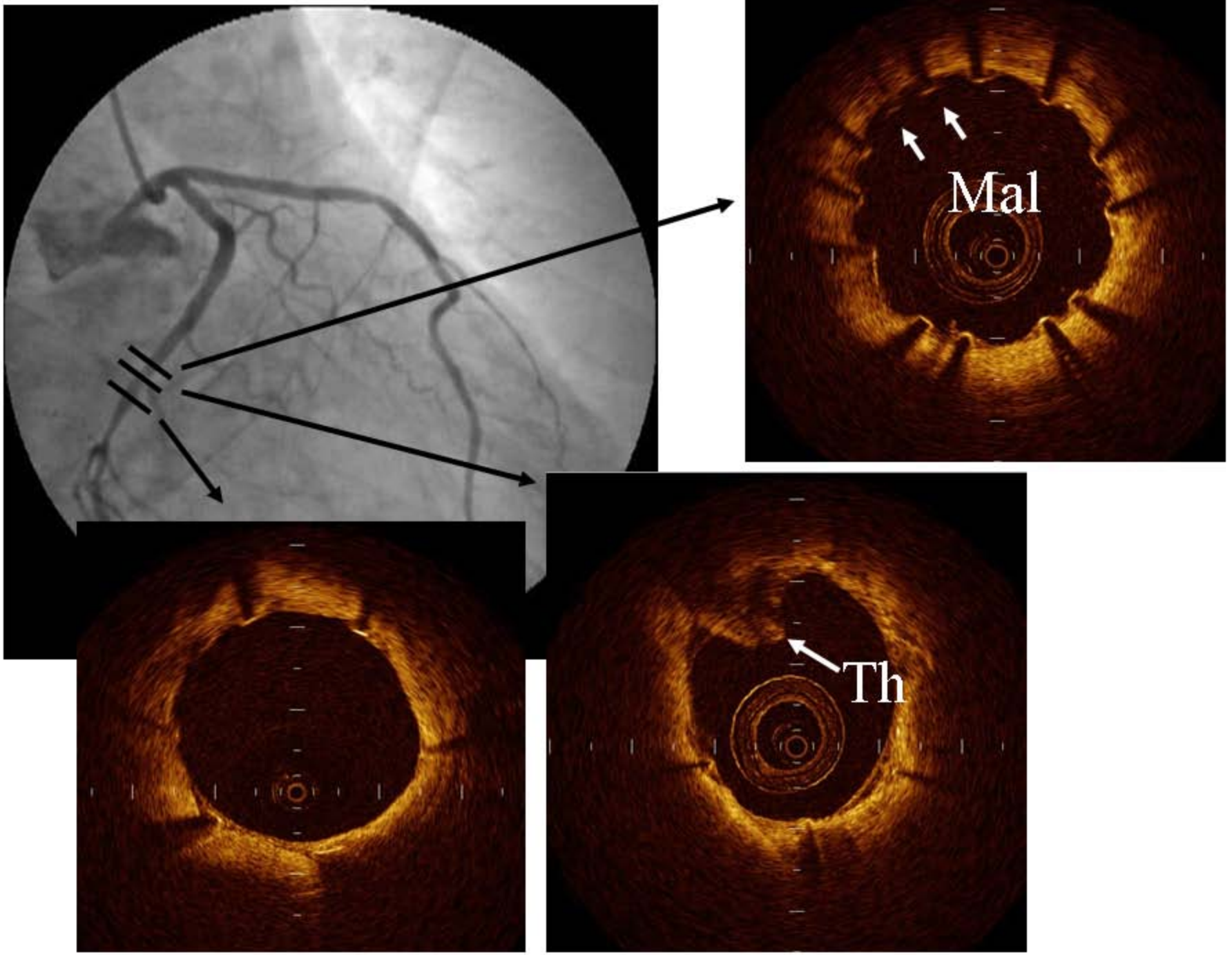
Mal
Th